Long-term stability of sharp Cu surface tips

V. Jansson,[*] E. Baibuz, and F. Djurabekova

Helsinki Institute of Physics and Department of Physics,
P.O. Box 43 (Pehr Kalms gata 2), FI-00014 University of Helsinki, Finland
(Dated: March 30, 2025)

Sharp nanoscale tips on metal surfaces of electrodes enhance locally applied electric fields. Strongly enhanced electric fields trigger electron field emission and atom evaporation from the apexes of the tips. Combined together, these processes may explain electric discharges in form of small local arcs observed near metal surfaces in the presence of electric fields even in ultra high vacuum conditions. In the present work we investigate the stability of nanoscale tips by means of computer simulations of surface diffusion processes on copper, the main material of high voltage electronics.

We study the stability and life-time of thin copper (Cu) surface tips at different temperatures in terms of diffusion processes. For this purpose, we have developed a surface Kinetic Monte Carlo model where the jump processes are described by tabulated precalculated energy barriers. We show that tall surface features with high aspect ratios can be fairly stable at room temperature. However, the stability was found to depend strongly on the temperature: 13 nm tips with the major axes in the $\langle 110 \rangle$ crystallographic directions were found to flatten down to half of the original height in less than 100 ns at temperatures close to the melting point, whereas no significant change in the height of these tips was observed after 10 μs at room temperature. Moreover, the tips built up along the $\langle 110 \rangle$ crystallographic directions were found significantly more stable than those oriented in the $\langle 100 \rangle$ or $\langle 111 \rangle$ crystallographic directions. The proposed Kinetic Monte Carlo model was validated against Molecular Dynamic simulation results via the comparison of the flattening times obtained by both methods. We also note that the Kinetic Monte Carlo simulations were two orders of magnitude computationally faster than the corresponding Molecular Dynamics calculations.

PACS numbers: 68.35.Fx, 68.47.De, 05.10.Ln, 07.05.Tp

I. INTRODUCTION

Vacuum arcs are local plasma discharges occurring in high electric fields in a vacuum environment[1]. The phenomenon has been observed to occur even in ultrahigh vacuum and constitutes a significant problem for high voltage or high gradient electromagnetic field devices. One of the examples of such demanding instruments is linear accelerators with high accelerating gradients, such as Compact LInear Collider (CLIC) under development at CERN.[2,3] The cause of vacuum arcs are still not properly understood, despite heavy efforts of both experimental and theoretical studies of the phenomenon.[1,4]

Experimental measurements of the field emission currents from a seemingly smooth surface suggest the existence of short-lived sharp and tall surfaces features (tips) that enhance the applied electric field explaining the β factor in the Fowler-Nordheim equation for field emission currents.[5–7] These are noticed to be precursors to electric arcs: breakdown events usually occur after electron currents reached the runaway values.[6] In the study by R. P. Little and W. T. Whitney, ~ 2 μm high pre-breakdown tips were observed with an aspect ratio of ~ 100 on copper cathodes, as well as on other metals[8]. Note that in these experiment the applied electric field was 10 MV/m and the vacuum 10^{-5} Pa (compared to the modern experimental setups, where the values of the electric fields are ≥ 100 MV/m and the vacuums $\sim 10^{-7}$ Pa).[9,10] However, no other studies to our knowledge have reported the observation of similar tips (see, e.g., Ref. 11) and mostly the field-emitting tips are associated with particles of a foreign origin or metal dust.[12,13] Unfortunately this hypothesis does not satisfactorily explain the experimental results obtained recently at CERN,[14] which confirms that the exact nature of the field-emitting tips still remains unknown. It is therefore of interest to use multiscale modeling to study how the surface behaves under high electric fields and, if any asperity emerged,[15] what is the life time of such an asperity after the electric field was removed.

We develop our model for copper (Cu) surface to match the material choice for the accelerating components of CLIC.[3] At the same time, Cu is a widely used material in many different high voltage devices. To date, there exist many Kinetic Monte Carlo (KMC) models for studying various processes on Cu surfaces, such as film growth due to deposition and surface roughening.[16–21] Atoms deposited on smooth metal surfaces tend to group together and form islands, which has been clearly observed by scanning tunneling microscopy.[22] Adatom islands were previously the objects of KMC studies, where the adatom migration energy barriers were either approximated by formulae based on bond-counting arguments,[23,24] or calculated on-the-fly by using self-learning algorithms.[20,25,26] The former method is fairly inaccurate and may only be effectively applied on relatively smooth surfaces, whereas the latter method is limited by its CPU-intensity. A bond-counting rule has been applied in a KMC study of surface asperities,[27] however, it was not validated against experiments nor any other methods.

Surface asperities with high aspect ratios, such as

tips, have a geometry and behavior similar to that of nanowires. The properties of the latter have also been studied intensively in both experiments and computer simulations, such as MD and KMC. For instance, the MD simulations of W. Liang et al. and H. S. Park et al. showed that thin nanowires oriented along the $\langle 100 \rangle$ crystallographic directions may spontaneously reconstruct the shape to align the major axis of the wire along the $\langle 110 \rangle$ direction.[28,29] Cu nanowires with diameters ~ 40 nm have also been seen experimentally to break the structural integrity during annealing at temperatures between 670 and 870 K, forming chains of spherical droplets.[30] This effect, known as the "pearling instability", was earlier predicted by KMC simulations of Ge nanowires by T. Müller et al.[30] and was explained by a variant of the Rayleigh instability mechanism.[31] The pearling effect has also been observed in ion-beam irradiated Au and Pt nanowires.[32] Large tips with a radius of about 120 nm and a height of more than 300 nm were, on the other hand, observed experimentally to be stable at room temperature for more than a month.[33]

In this paper, we study the stability and life-time of thin Cu surface tips in terms of diffusion processes of atoms on metal surfaces. For this purpose, we have developed an atomistic Kinetic Monte Carlo model. The model consists of the KMC code *Kimocs*, which is described in Sec. II A, and the parameterization of the Cu surface diffusion processes, described in Sec. III. The validation of the model is described in Sec. IV A, where the processes of flattening of small asperities on {110}, {111}, and {100} surfaces, and at different temperatures, are compared with corresponding Molecular Dynamics simulations. In Sec. IV B, the model is used to investigate the stability and the life time of 13–31 nm high tips on different Cu surfaces and at different temperatures. Finally, we discuss the results in Sec. V and summarize our conclusions in Sec. VI.

II. COMPUTATION METHODS

A. Kinetic Monte Carlo

We present a newly developed atomistic KMC code, *Kimocs*, for simulating the evolution of metal surfaces on the atomic scale. In *Kimocs*, a rigid face-centered-cubic (fcc) lattice is assumed. The lattice spans the whole simulation system, including bulk, surface and vacuum space above the surface (see Fig. 1). At every KMC step, one atom may jump to an unoccupied first nearest neighbor (1nn) lattice site with a precalculated transition rate, in accordance with the general KMC algorithm.[34–36] Atom jump processes are thermally activated and their transition rates Γ are thus given by the Arrhenius formula:

$$\Gamma = \nu \exp\left(\frac{-E_m}{k_B T}\right), \qquad (1)$$
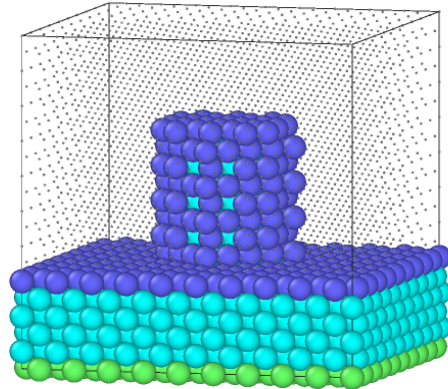
where

FIG. 1. (Color online) In *Kimocs*, the atoms have to assume the positions on a rigid lattice (dots). Only the atoms with one or more unoccupied first nearest neighbor sites may migrate (blue), as opposed to the atoms that are fully surrounded by other atoms (cyan). Atoms at the lower boundary (green) may be permanently fixed to account for infinite bulk.

- ν is the attempt frequency of the process
- k_B is the Boltzmann constant
- T is the temperature of the system
- E_m is the migration energy (or activation energy) of the atom to move from one lattice point to another

In *Kimocs*, all atom jump processes are characterized by the number of the first nearest neighbor and the second nearest neighbor (2nn) atoms in the three-dimensional space of the initial and final sites, as shown in Fig. 2. We denote the number of 1nn and 2nn atoms of the initial site as a and b, respectively, and the corresponding numbers for the final site as c and d. Then, the migration energy of the jump process is described by four indices: $E_m(a, b, c, d)$. In the fcc lattice, the indices a and c are between 0 and 12, whereas the indices b and d are between 0 and 6. The values of $E_m(a, b, c, d)$ are precalculated and tabulated (see Sec. III).

In *Kimocs*, the fcc lattice, and thus the atoms, may be arranged in three different orientations, allowing for three different surfaces: {100}, {110}, and {111}. The boundary conditions may be periodic in all three directions: x and y (lateral directions), and z (upwards). With non-periodic boundaries in the z direction, the atoms that reach the upper boundary are removed, whereas the atoms in the bottom layer are assumed to belong in the bulk and thus fixed.

The time increment at each KMC step is calculated according to the residence time algorithm,[35]
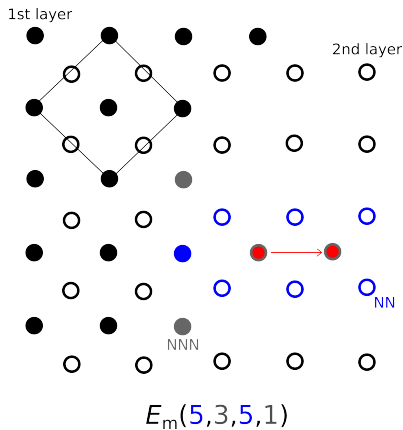
$$\Delta t = \frac{-\log u}{\sum_i \Gamma_i}, \qquad (2)$$

FIG. 2. (Color online) Illustration of the characterization of an atom migration jump on a {100} surface in *Kimocs* (between the two sites marked in red). Two atom layers are shown: the first layer (top, shown with filled circles) and the second layer (below, empty circles). The first nearest neighbor (1nn) sites are marked blue and the second nearest neighbor (2nn) sites gray. Note that the migrating atom is counted as one of the 1nn atoms of the final (initially empty) site. To guide the eye, the face-centered cubic (fcc) unit cell is shown by black lines.

where the sum is taken over all possible events i at a certain state of the simulation and $u \in (0, 1]$ is a uniform random number.

B. Nudged Elastic Band

For calculating the atom migration energy barriers, the minimum energy path was found by using the Nudged Elastic Band (NEB) method[37,38] with the MD code PARCAS.[39–41] The atomic systems for the initial and final states were constructed by *Kimocs*. These systems had the dimensions presented in Table I. The bottom layer atoms were fixed. The initial and final states were relaxed using the conjugate gradient method. By linear interpolation between the atom positions of the initial and final states, 40 images were created. These images were used for the NEB calculation with PARCAS. Periodic boundaries in lateral x and y directions along the surface were used. No temperature nor pressure controls were used.

For the NEB calculations and MD simulations, we chose the interatomic potential based on the Corrected Effective Medium Theory (CEM), developed by M. S. Stave et al.[42] The potential has been proven to be suitable for modeling of Cu surfaces.[43] For instance, the potential predicts the the {111} surface to be the most stable with the surface energy 1.76 J/m^2, while the surface energies of {100} and {110} are 1.91 J/m^2, and 2.08 J/m^2, respectively.[43] For comparison, DFT gives 1.952 J/m^2 for {111}, 2.166 J/m^2 for {100}, and 2.237 J/m^2 for the {110} surface.[44] The experimental value of the surface energy for the {111} surface was reported to be $\sim$1.8 J/m^2.[45,46] As one can see, the surface energies given

TABLE I. The dimensions used for the simulated systems with different surfaces and the number of atomic monolayers (ML) used for the substrate. The z direction is normal to the surface.

Surface	x [nm]	y [nm]	z [nm]	Substrate [ML]
{100}	7.4	7.4	14.8	12
{110}	12.8	9.0	5.2	18
{111}	9.0	5.2	12.8	30

by the CEM potential are in good agreement with both DFT and experiments.

C. Molecular Dynamics simulations

We have also perform benchmarking MD simulations by using the PARCAS code[39–41] with neither pressure nor temperature control. The dimensions of the simulation cells and the number of atoms were selected to match the ones used in *Kimocs*. Periodic boundary conditions where used in x and y directions, but not in z. The bottom layer atoms were fixed. The CEM potential for Cu,[42] which was used to calculate the barriers, was used also in the MD simulations. The simulations were performed with the time step 4.06 fs until the surface tip had flattened down to half of its initial height; i.e., the simulations stopped when no atoms were above a certain z coordinate.

III. PARAMETERIZATION OF THE KMC MODEL

The parameterization of the Cu material, which we used for our model, can be summarized as follows:

- The migration energy barriers are calculated using the NEB method;

- Processes involving atoms in unstable initial or/and final positions are treated separately. These positions may only appear due to the adopted rigid lattice approach and are usually parts of multiple transitions.

- The attempt frequency ν is estimated from a fit to corresponding MD data

These points will be described in detail in the following three subsections.

A. Migration barrier calculations

The evolution of the simulated system in *Kimocs* is driven by diffusion jumps by atoms from occupied (initial) sites to unoccupied (final) ones in the 1nn vicinity of the former. Each jump in the system is associated

with an energy barrier, $E_m(a, b, c, d)$, where a, b, c, and d are the number of 1nn and 2nn atoms in the initial and final states (for details, see Sec. II A). The values of $E_m(a, b, c, d)$ are calculated using the NEB method implemented within the MD code PARCAS.[39–41] The intrinsic feature of the adopted model assigns the value of $E_m(a, b, c, d)$, calculated for the randomly selected positional configuration described by the a, b, c, and d indices, to all processes with the same set of these values. Although these identically interpreted transitions, which differ from one another by configurational arrangement only, may have slightly different energy barriers, we currently neglect these differences for the sake of computational efficiency. An exact description of the 1nn atom jumps with all positional permutations included would require about 10^7 barriers to be calculated. However, ignoring the permutations and classifying all the transitions only by the (a, b, c, d) indices, the number of required calculations is reduced by several orders of magnitude.

We used the following algorithm to calculate the migration barriers. For representative positional permutations of a certain (a, b, c, d) transition, we recorded possible situations which were probable to occur in the atomic system of interest by running *Kimocs* for populations of randomly distributed adatoms on {100}, {110}, or {111} Cu surfaces. We also used a bulk system with a random distribution of vacancies to characterize the processes with a high number of 1nn and 2nn atoms.

The values of the migration barriers were calculated as follows. Firstly, the initial and final states of the atomic systems for a given transition (an atom jump) were relaxed using the conjugate gradient method. After that the minimum energy path for the jumping atom to perform the transition between the initial and final states was found using the NEB method. The energy barrier, $E_m(a, b, c, d)$, was defined as the difference between the saddle point (the potential energy maximum) of the minimum energy path and the potential energy of the initial state. These energy barrier values were then added to the database to be used in *Kimocs* for the actual simulations.

We estimated the uncertainty of the barrier values obtained by using the proposed (a, b, c, d) characterization. We calculated the energy barriers for different jump processes identified with the same (a, b, c, d) values, as is the case for, e.g., the processes shown in Fig. 3. On average, five different permutations were calculated for 196 different (a, b, c, d) transitions on a perfect {100} surface with randomly distributed adatoms. The average standard deviation of the energy barriers for these 196 configurations was found to be 0.13 eV or 14.8 %, which gives an indication of the precision of our energy barrier characterization and subsequently of our KMC model in general.

It is also possible in some cases that the atoms in the 1nn or 2nn positions move to different positions during the relaxation by the NEB method. If this happens, the NEB calculation is discarded, as the obtained value of the energy barrier would not correspond to the sought
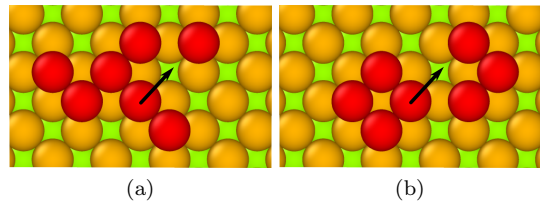

(a)   (b)

FIG. 3. (Color online) Two different permutations of the $(6, 3, 7, 3)$ atom jump process.

(a, b, c, d) transition, but another process which is described by the (a, b, c, d) indices corresponding to the states where the jumping atom found itself after the relaxations. During the calculations we also encountered situations in which the atoms were relaxing into different final positions than the expected ones. In these situations we ignored the exact position while calculating the barriers since only the values of the potential energies in the saddle point and the initial state were important.

In principle, the small nanosize surface features must be studied by taking into consideration the finite-size effect due to the large surface areas with respect to the atoms in the bulk of the nanotips, which may affect dramatically the material properties. For instance, the melting point of thin nanowires has been shown to drop rapidly when the diameter of nanowire was below 20 nm.[47] In the same reference it was shown that 1 nm thick nanowires may melt already at room temperature. Although this process is well captured by the used CEM potential, this effect is currently not introduced in our model. The problem with unstable neighbor atoms was accentuated for migration barrier calculations on small nanotips, as the whole structure was much less stable during the relaxation process. Therefore, more robust systems such as plane surfaces or voids in the bulk, were preferred for the barrier calculations.

B. Transitions involving atoms in unstable positions

We noticed that atoms with no more than three 1nn atoms ($a \leq 3$) have near zero migration barriers to perform jumps to any other 1nn position. These processes take place instantaneously and are thus spontaneous. In the terminology of *Kimocs*, these atoms are said to be in unstable positions. To avoid the zero barrier problem, we apply a very small migration energy barrier to imitate the spontaneous jumps of unstable atoms:

$$E_m(a, b, c, d) = \epsilon a + \delta b + \epsilon c^{-1} + \delta d^{-1} \qquad (3)$$

where $a \leq 3$. Although the differences are not expected to be large, this formula gives a priority to unstable atoms with less neighbors to jump before the unstable atoms with more neighbors. We assume that an atom jump to a

position with a higher number of neighbors is more favorable: higher a and b thus raise the barrier, whereas higher c and d lowers it. We also take into account that 1nn atoms contribute stronger in the value of migration barriers compared to 2nn atoms by setting the corresponding contributions $\epsilon = 10^{-3}$ eV and $\delta = 10^{-4}$ eV for the 1nn and 2nn atoms, respectively, in order to obtain the right trend. Using these parameters, the maximum migration energy for an unstable atom is $E_m(3, 6, 1, 1) = 0.0047$ eV, which is insignificant compared to even thermal energies (~ 0.025 eV). This is why the processes described by these barriers will appear spontaneous in the simulations. The low energy barriers ensure that the time increments, calculated by Eq. 2, are not overestimated.

C. The attempt frequency

Another important parameter for KMC simulations is the attempt frequency ν for a jump to happen (see Eq. 1). This parameter affects the time predicted for a studied process to be completed. Since all processes in our model are jumps by atoms to 1nn lattice sites, the attempt frequencies can be reasonably assumed to be approximately the same for all transitions. It is also frequently assumed to be of the same order of magnitude as the Debye frequency (for Cu, $\nu = 4.5 \cdot 10^{13}$ s^{-1}).[48–52] In our model we fitted the value ν to the MD simulations (for simulation details, see Sec. II C), comparing the flattening time of a surface tip obtained by both methods. The fitting procedure can be described as follows.

A small cuboid tip with 576 atoms and a height of 12 monolayers (ML) were placed on three different Cu surfaces: {110}, {111}, and {100}, respectively. The system dimensions are listed in Table II. Periodic boundaries were used in the lateral x and y directions. The bottom layer of atoms was fixed and monitored throughout the simulations not to interact with the jumping atoms of the surface. The time elapsed for the cuboid tip to flatten down in height from 12 to 6 ML at 1000 K with different attempt frequencies was recorded. The statistical uncertainty was taken into account by using ten different seed numbers for every value of the attempt frequency. The obtained flattening times are plotted in Fig. 4 and compared with the average MD values (the tabulated values and discussions can be found in Sec. IV A 1). By fitting the KMC data to the MD values, we found that the attempt frequency value belong in the range between $7 \cdot 10^{13}$ s^{-1} and $2 \cdot 10^{14}$ s^{-1}. We chose $\nu = 7 \cdot 10^{13}$ s^{-1}, as it is closer to the Debye frequency value of Cu.

TABLE II. The dimensions of different simulation cells with three different surface directions used for determining the attempt frequency in MD and KMC. The number of atom monolayers (ML) indicates the thickness of the substrate, on which the tip was placed. The z dimension is normal to the surface.

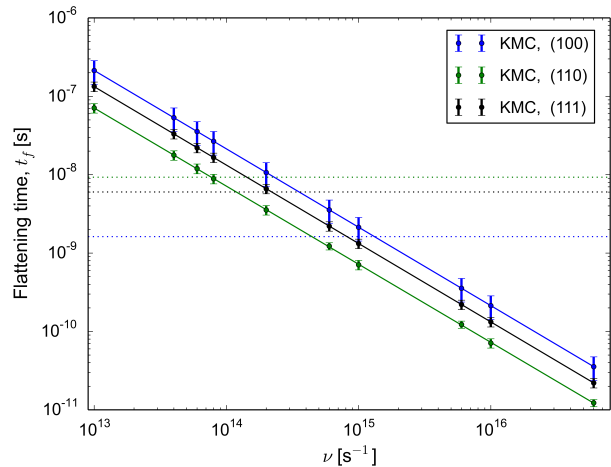| Surface	x [nm]	y [nm]	z [nm]	Substrate [ML]
{100}	7.4	7.4	14.8	12
{110}	12.8	9.0	5.2	18
{111}	9.0	7.8	12.8	30

FIG. 4. (Color online) The flattening time for the simulated 12 ML tip as a function of the attempt frequency used in *Kimocs*. The flattening time is calculated as the time elapsed for the tip to flatten down in height from 12 to 6 ML. Three different surfaces (lattice orientations) were used: {100}, {110} and {111}. The dotted lines indicate the flattening times obtained in MD simulations (for tabulated values, see Table III).

IV. RESULTS

A. Validation of the model

1. Flattening time with different surfaces

Using the parameterization described in Sec. III, we carried out a series of *Kimocs* simulations to validate our model against corresponding MD simulations. At first we analyzed the flattening process of 12 ML high cuboid surface tips with respect to the crystallographic orientation of the surface. The details of the simulation setups are the same as in Sec. III C. The temperature was set to 1000 K and the simulations were stopped when the height of the cuboid tips had decreased to 6 ML (half of their original size). The simulations were repeated with ten different seeds and the average flattening time was recorded for each surface, as seen in Table III. In order to validate the KMC model, the results have been compared with Molecular Dynamics (MD) simulations, as also shown in

TABLE III. Flattening of cuboid tips, 12 ML high with 576 atoms, on different surfaces at 1000 K; comparing MD and KMC. The simulations were stopped when the tips had flatten below half their original height (6 ML).

Surface	MD [ns]	KMC [ns]
{110}	9.29 ± 1.44	9.25 ± 1.10
{111}	6.01 ± 1.48	18.8 ± 0.96
{100}	1.62 ± 0.60	31.0 ± 6.61

Table III and Fig. 5. The results of the KMC simulations agrees with the MD results with a factor of less than 20. We also note that the KMC simulations were two orders of magnitude faster computationally than the MD simulations.

The results presented in Table III show a very good agreement between the results obtained with KMC and MD for the tips built on a {110} surface as they are the most stable ones. The tips built on the {111} and on {100} surfaces compare worse, which can be explained by the shape transformations of small scale (diameter ~ 2 nm) tips. These transformations are seen in MD simulations,[28,29] but not accessible by KMC due to the assumed rigid lattice of the simulated material. However, overall the agreement is fairly good and does not exceed the factor 20, taking into account the different nature of the two simulation techniques (no relaxation of the lattice is taken into account in KMC, also the barriers for other than the {111} surfaces can be overestimated by NEB)

2. Flattening time with different temperatures

Analysis of the flattening time over the range of temperatures will enable the prediction of the stability of the small size tips at much lower temperatures (room and below), which are difficult to access even by KMC methods. For this, we repeated the same KMC simulations as in Sec. IV A 1 with temperatures ranging from 500 to 1200 K. For comparison, MD simulations of the same systems were performed for a temperature range of 850 to 1200 K. The KMC data points from 900 K and higher were averaged over 10 runs per temperature, whereas the data points for lower temperatures were performed only once. The simulations were stopped when the cuboid had been flatten down to below half its original height (6 ML). The flattening time t_f was found to follow Arrhenius-like behavior:

$$t_f = t_0 \exp\left(\frac{E_a}{k_B T}\right), \qquad (4)$$

where the prefactor is $t_0 = 2.34 \cdot 10^{-12}$ s, the activation energy is $E_a = 0.72$ eV, and k_B is the Boltzmann constant. These can be compared to the values fitted to the MD data: $t_0 = 7.33 \cdot 10^{-14}$ s and $E_f = 1.00$ eV. Both sets

of t_0 and E_a compare well to the average migration barrier and inverse of the attempt frequency of the diffusion jumps (1.04 eV and $1.4 \cdot 10^{-14}$, respectively).

The results are plotted in Fig. 6. At temperatures between 800 and 1100 we see a very good agreement of the KMC and MD results. The temperature dependence for the flattening time clearly shows the same trend in both methods. The KMC model slightly overestimates the flattening time compared to MD near the melting temperature of Cu, 1357.8 K.[54] At the low temperatures (below 850 K), the comparison is not possible, since MD is too slow to produce any sensible data in this regime. The dashed line is an extrapolation obtained by fitting the formula, Eq. 4, to the MD data (filled squares).

3. Adatom islands

We have also analyzed the migration of single adatoms on the surface to assess whether the model can capture satisfactorily the surface diffusion on Cu surfaces. We studied the dynamics of adatom migration by distributing randomly 300 adatoms on an atomically smooth surface. Three different surfaces were considered: {100}, {110}, and {111}. The dimensions of the surfaces were 10×10 nm^2. We saw that adatom islands were formed in less than 1 ns on all three surfaces. Moreover, the bigger islands were growing on the expense of smaller ones following the Ostwald ripening mechanism: the islands grew larger over time as their number became smaller.

In Fig.7 we show examples of the nanoislands formed on all three different surfaces. As one can see the faster diffusion process on the {111} surface results in clearly separated and well defined big islands. The {110} surface exhibits the least pronounced structure as the preferential migration along $\langle 110 \rangle$ surface channels leads to the formation of elongated and less organized structures.

The adatom island dynamics produced by our KMC model is thus in good agreement with experiments[22] and other KMC studies.[23,25,26]

B. Stability of large tips

1. The flattening process for large tips

Tall and sharp surface tips with high aspect ratios are believed to be responsible for the enhanced field emissions and vacuum arcs observed in experiments with high electric fields[5–7]. The exact shape of these tips and how they are created is not known. Tips are not likely to be seen after vacuum arc events. It is also quite difficult to observe tips which may have grown under an electric field but have not yet caused a vacuum arc. No such evidences exist in the literature to our knowledge. It suggests that the life time of such tips is too short to be observed with electron microscopes or other experimental techniques. Using our KMC model, we have simulated the flattening
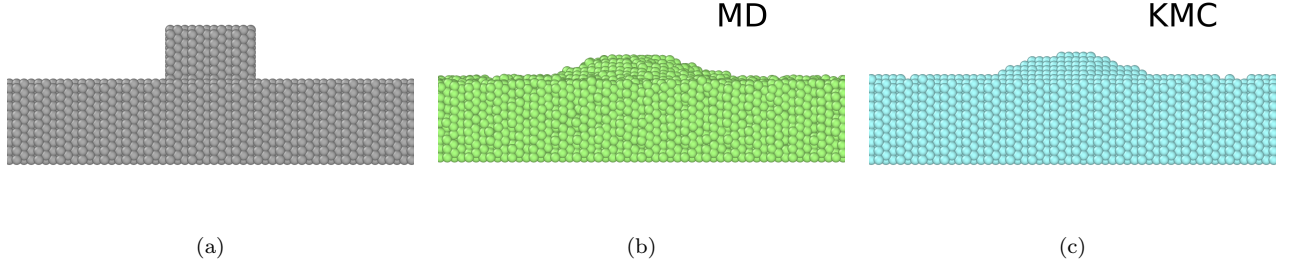
(a) (b) (c)

FIG. 5. (Color online) Final snapshots of MD (b) and KMC (c) simulations of flattening of a 12 ML tip, initially in the shape of a cuboid (a). In both methods the simulations were stopped when the tip height was reduced by half. The surface evolutions predicted by both methods are identical (see comparative animation in the Supplementary Material[53]).
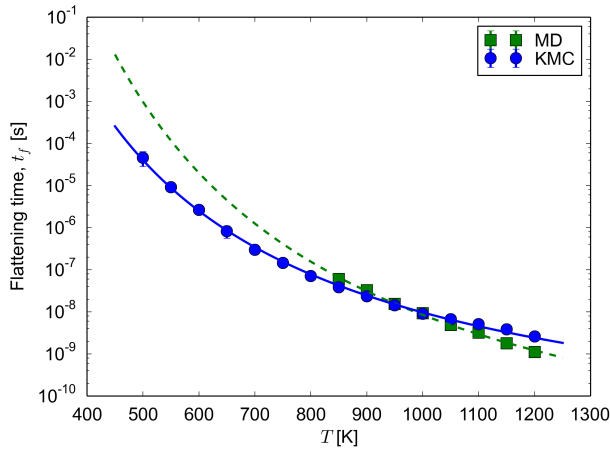

FIG. 6. (Color online) Flattening time with KMC and MD for a cuboid tip with a height of 12 ML (1.6 nm) and 576 atoms on a {110} surface as a function of temperature. The lines are the fits of Eq. 4 to the KMC (solid) and MD (dashed) results.

(a){100}

(b){111}

(c){110}

FIG. 7. (Color online) Coalescence of adatoms resulting in nanoislands on the {100}, {111}, and {110} surfaces.

process of large narrow tips that may be considered as candidates for field-emitting tips. By estimating the flattening time of the tips at different temperatures, we have evaluated the stability and life time of field-emitting tips.

The flattening time of a cuboid tip built on a {110} orientated Cu surface was estimated using our KMC model. The height of the tip was 13 nm and the width 2 nm, resulting in an aspect ratio of ∼7. Consistently with our previous simulations, we continued the simulations of the tall tips until they shortened to the half of their original height, 7 nm. We simulated the tips at different temperatures between 800 K and 1200 K. The results are shown in Fig. 8.

In Fig. 9 we show the sequence of images (snapshots taken at 0.0 μs, 0.2 μs, 2.1 μs, and 6.3 μs of simulated time) of the flattening process of the tip at 1200 K. We see that the main mechanism for flattening is the diffusion of atoms down from the sides of the tip
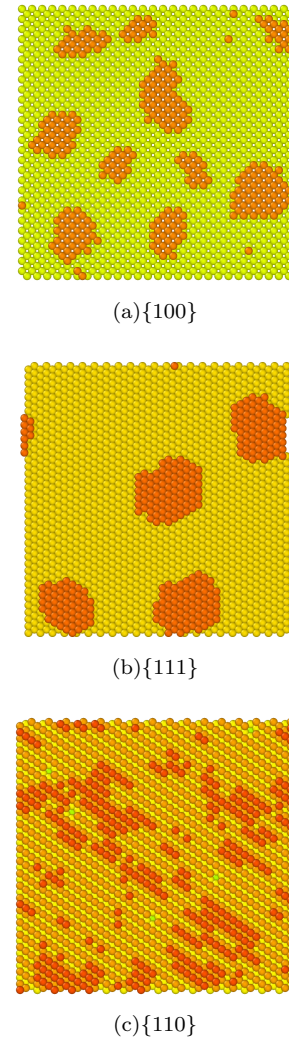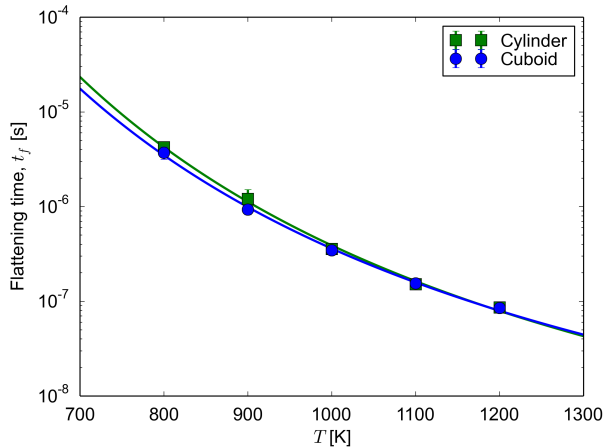
FIG. 8. (Color online) Flattening time for large 13 nm high tips versus temperature. The simulations were stopped when the height of the tip was reduced to the half of its original size.

to the substrate. At first, the close-packed {111} facets are formed on the tip sides, as shown in Fig. 10. This process stabilizes the tip as the atoms have more neighbors (bonds) within the plane, whereas the adatoms migrating on this plane have less bonds and thus migrate more easily. These facets then shrink layer by layer, as also these atoms diffuse towards the substrate. As in the case of the small tips in Sec. IV A 2, the flattening time again follows an Arrhenius-like trend (Eq. 4) with a prefactor $t_0 = 1.43 \cdot 10^{-11}$ s and an activation energy of $E_a = 0.89$ eV. The value of the activation barrier is greater in this case, which is explained by the strong faceting of the taller tips. The taller the tip the more atoms are bonded in the closed-packed facets, and hence a higher migration energy is required for the atoms to break out of the faceted plane and diffuse.

At 300 K, no significant change of the tip was observed after 10 μs. Using Eq. 4, the flattening time at 300 K can be estimated to 3.1 h. The faceting of the substrate is an artifact of the periodic boundary condition and is not the result of the current model.

We also repeated the same simulations with cylindrical tips instead of cuboids. The cylindrical tips had the same height, 13 nm, and number of atoms, 4800, as in the case of the cuboid tip. No significant difference in the flattening time was observed (see Fig. 8).

2. The pearling instability for tips and nanowires

During the simulations of tall tips on the {100} and {111} surfaces we found that they were unstable at 1000 K with our KMC model. The tips were 13 nm high with a diameter of 2.6 nm. At 1000 K, the tip with the major axis in the ⟨100⟩ direction exhibited Rayleigh necking and separated from the substrate after 70 ns. After

400 ns, the detached tip had changed into two barely attached polygon-shaped crystals [see Fig. 11(a)]. The tip oriented in the ⟨111⟩ direction also exhibited necking and detached from the surface after 100 ns. The remainder of the suspended (not attached to the substrate) tip developed regular facets but was stable for at least another 300 ns [see Fig. 11(b)]. A larger ⟨111⟩ tip of the height 32 nm and the diameter 1.8 nm also necked at the surface, but the upper part of the tip, which also developed regular facets as the smaller tip, remained stable for at least 900 ns [see Fig. 11(c)]. This kind of Rayleigh instability is similar to the "pearling instability" effect that has been observed experimentally for Cu nanowires.[30,32,55] We also repeated the simulations for the 13 nm high ⟨100⟩ and ⟨111⟩ tip systems with the substrate removed and periodic boundary conditions added in the z direction; thus creating infinitely long nanowires. The same necking behavior was observed for the wires as for the corresponding tips.

V. DISCUSSION

A. The model

The key assumptions of our model are that the surface diffusion processes can be correctly described by atom jumps to 1nn positions and that these jumping processes and the associated migration energy, E_m, can be characterized solely by the number of 1nn and 2nn atoms of the initial and final positions (a, b, c, d), as described in Sec. II. Jumps to 2nn sites and concerted movements, where more than one atom move at once, are not considered in the model.

The model also assumes all atoms always belong to either the surface or the bulk; jumps to the vacuum above the surface are currently forbidden and evaporation is not considered. Even if clusters detach during the simulation from the main simulation cell, each cluster is considered by *Kimocs* as an independent system; there are no gravitational or other forces implemented that would move a detached cluster as a whole, as would be physically expected. Atoms in the detached cluster may only jump one at a time, as specified by the KMC algorithm.

B. The parameterization of Cu

The migration barriers for all jump processes were calculated using NEB, which is commonly used for finding the energetically most favorable migration path. Since our parameterization depends on the number of neighbors of the jumping atom, the NEB calculations had to be discarded if any neighbor atoms moved during the relaxation of the system as the resulting barrier would not be calculated for the desired process any more. In particular, we found that atoms with less than 4 atoms in
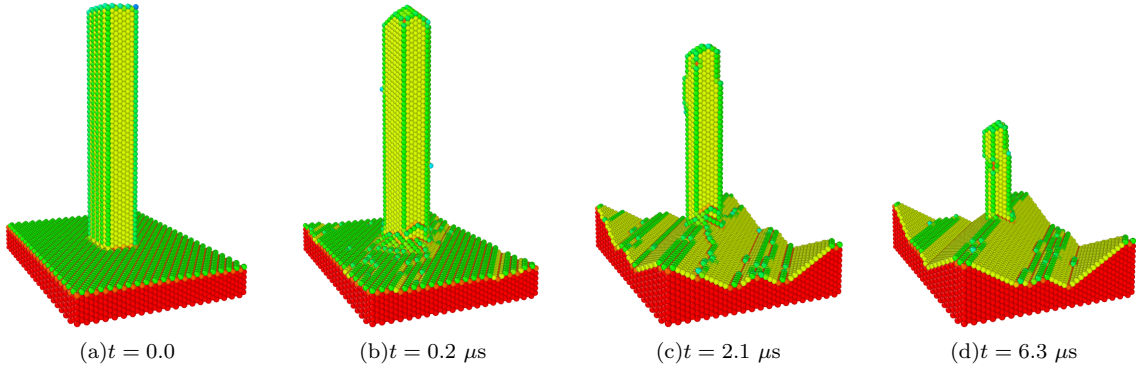
(a)$t = 0.0$ (b)$t = 0.2$ μs   (c)$t = 2.1$ μs   (d)$t = 6.3$ μs

FIG. 9. (Color online) The flattening of a 13 nm high tip at 1200 K at (a) $t = 0.0$, (b) after 0.2 μs, (c) after 2.1 μs, and (d) after 6.3 μs, when it was reduced to half of its original height. The atoms are colored according to their coordination number (amount of 1nn atoms) to highlight the faceting of the tip. The tip is initially a cuboid with a {110} top surface and two {112} and {111} side surfaces (See Fig. 10 for a detailed view). Already after 0.2 μs, the closed-packed {111} facets (yellow) are dominating and the {112} facets have disappeared. The ridges formed on the substrate surface is an artifact caused by the periodic boundary conditions.
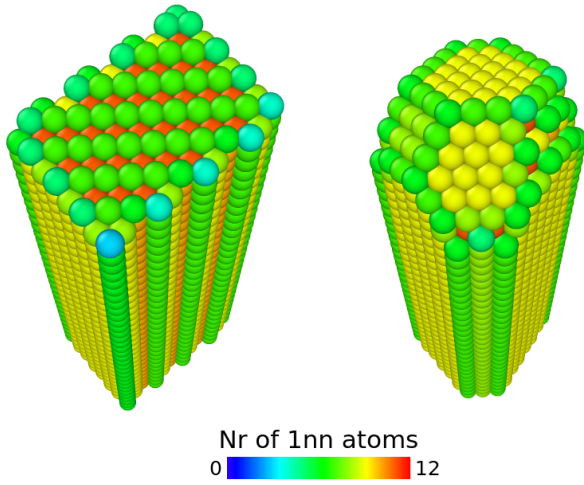

Nr of 1nn atoms

0 ▮ 12

FIG. 10. (Color online) Detailed view of the apex of the 13 nm tip in Fig. 9 at $t = 0.0$ (left) and $t = 0.2$ μs (right). The atoms are colored according to their coordination numbers. The surface atoms become more bonded (due to the faceting) in the course of the simulation.

the 1nn positions are very likely to move during the relaxation (and are thus in unstable positions). A similar result was found for aluminium in Ref. 56, were atoms with less than 3 atoms in the 1nn positions were found to be unstable in atomistic simulations.

All atoms with less than 4 neighbors in the 1nn positions will have zero or near-zero energy barriers for jumps. Although for simplicity, a single small barrier

value for these jumps could have been assumed, it may lead to an undesired choice for a jump of the atom which has a very few bonds but still slightly stronger bonded than its neighboring atom with even less bonds. For instance, having many atoms with few neighbors next to one another might result in an atom jumping to a more bonded position, leaving behind an atom with no nearest neighbors. This will lead to disintegration of the structure and, moreover, violate the principle of KMC. Thus the less stable atom must be given priority to perform the jump. To cope with this problem, we propose Eq. 3. It is designed to give near-zero barriers for unstable atoms, but the less bonded atoms will, however, have even smaller barriers. This way the integrity of the surface is ensured and the barriers given by Eq. 3 do not affect the overall dynamics of the system or the time estimation in Eq. 2.

Since we only consider atom jumps to 1nn positions, it is fairly reasonable to assume the same attempt frequency ν for all processes. In our model we have fitted the value of ν, which resulted in the same flattening time for the surface tip as obtained with MD simulations (see Sec. III C). Slightly different flattening times are obtained for different surfaces with MD, as seen in Table III. It has been found in other MD studies that wires with a $\langle 100 \rangle$ orientation will easily undergo a transition to a $\langle 110 \rangle$ orientation.[28,29] We note that the $\langle 100 \rangle$ to $\langle 110 \rangle$ lattice transition is not possible on a rigid lattice, as in the *Kimocs* model, since a large part of the nanowire lattice must change orientation in a concerted movement. *Kimocs* will not account for this transition, which explains the large discrepancy between the KMC flattening time for a $\langle 100 \rangle$ oriented tip and the MD results. For the fitting of ν, the {110} and {111} systems are thus the most reliable and ν is found to be between $7 \cdot 10^{13}$ s^{-1} and $2 \cdot 10^{14}$ s^{-1}. The chosen value of $\nu = 7 \cdot 10^{13}$ s^{-1} is the
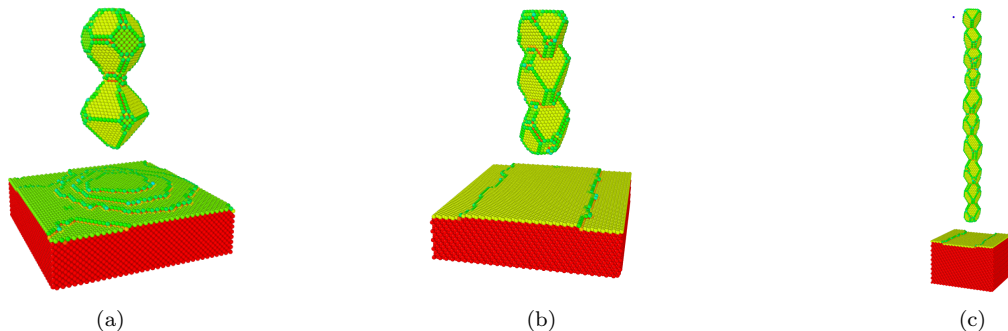
FIG. 11. (Color online) The necking instability of a 13 nm high tip at 1000 K with $\langle 100 \rangle$ orientation after 400 ns (a), the same for a $\langle 111 \rangle$ tip of identical height after 300 ns (b). The $\langle 111 \rangle$ tend to neck near the substrate, whereas the broken-off structure obtains a regular faceted pattern that keeps stable also after 900 ns, as shown in (c) for a 31 nm high $\langle 111 \rangle$ tip. The atoms are colored according to their coordination number in order to highlight the faceted structures.

nearest to the Debye frequency, $4.5 \cdot 10^{13}$ s^{-1}, as often assumed in the KMC community.[48–52] This value gives an overestimation of the flattening time with a factor 3 for the $\langle 111 \rangle$ tip and a factor 20 for the $\langle 100 \rangle$ tip (see Sec. IV A 1, Table III), which is acceptable.

The KMC data agree well with MD results at temperatures > 800 K, but the trend differs a bit. However, we do not have MD data to compare with below 850 K, as the MD method becomes too slow at low temperatures. The extrapolation of the MD data indicates that the flattening time might be much longer than the 3.1 h predicted by KMC.

By considering the dynamic behavior of the KMC simulations, we can conclude that the general evolution of the atomic system, as observed in MD simulations, is well reproduced in the case of the flattening of small tips (see Fig. 5). The coalescence of adatoms into islands, as seen in experiments and other KMC models,[22] is also correctly reproduced. For the {111} surface, one limitation of our model to take into account is that adatoms may not take hcp positions, as discussed in Ref. 26, as the model only allows fcc positions.

C. The stability of large tips

The KMC simulations of large surface tips with aspect ratios of ∼7 show that tips with the $\langle 110 \rangle$ orientation are particularly stable compared with tips of the $\langle 100 \rangle$ or $\langle 111 \rangle$ orientations. The latter ones are susceptible to the "pearling instability",[30,32,55] i.e., breaking into pieces due to Rayleigh necking. In the simulations with the pearling effect, it should be noted that no gravitational nor other external forces, are taken into account; the pieces detached from the bulk remain suspended in vacuum as an entity in this KMC model. We also note that nanowires with a thickness of 1.8–2.6 nm will have a reduced melting temperature of 900–1000 K due to the finite size effect,[47] which is not taken into account in the KMC model. Nor is a rigid lattice KMC model able to

properly handle melting processes. We are nevertheless able to observe the Rayleigh instability with our model. High temperatures in KMC lead to the liquid-like behavior of surface atoms, since all jumps become almost equally possible, the kinetics of the process leads to the formation of thermodynamically favorable surface structures. The present result can be considered as the maximal temperature limit of the duration of the nanotips.

Our simulations show that there is no significant difference in the stability of a cuboid tip, compared to a cylindrical tips with the same height and number of atoms, which can be relevant for the small scale features. It should be noted that the thickness and height of the tip will affect the flattening time, as already seen in KMC studies of smaller Cu surface structures by Frantz et al.[27] However, according the our simulations, given a constant room temperature, nanoscale Cu tips with aspect ratios even as high as ∼7 will be stable for several hours if they have a $\langle 110 \rangle$ orientation and only diffusion processes are considered.

VI. CONCLUSIONS

We have developed a Kinetic Monte Carlo model for the long-term surface evolution of Cu. The model considers atom jumps to first nearest neighbor lattice sites on a rigid lattice. The jumps are characterized by the number of first and second nearest neighbor atoms of the initial and final sites. The model was validated by comparing flattening times of Cu surface tips with Molecular Dynamics results for three different surfaces and different temperatures. The computational speed was two orders of magnitude higher with our model than with Molecular Dynamics.

Tips with a $\langle 110 \rangle$ orientation were found to be significantly more stable than those with $\langle 111 \rangle$ or $\langle 100 \rangle$ orientations. The stability of tips were found to increase strongly with decreased temperature and a 13 nm high tip with an aspect ratio of ∼7 can be expected to be stable for

hours at room temperature. However, at temperatures near the melting point, such a tip will be reduced to half of its height in less than 100 nanoseconds. The life time of a field emitter in the shape of a tip with a large aspect ratio can therefore be assumed to be considerably sensitive to the temperature already by considering the surface diffusion processes alone.

ACKNOWLEDGMENTS

The authors would like to thank Antti Kuronen for providing his implementation of the NEB method for

* Email: ville.b.c.jansson@gmail.com

[1] P. J. Boxman, Raymond L.and Martin and D. M. Sanders, *Handbook of vacuum arc science and technology: fundamentals and applications /* (Noyes Publications, Park Ridge, cop. 1995.).

[2] H. Timkó, *Modelling vacuum arcs: From plasma initiation to surface interactions*, Ph.D. thesis, University of Helsinki (2011).

[3] M. Aicheler, P. Burrows, M. Draper, T. Garvey, P. Lebrun, K. Peach, N. Phinney, H. Schmickler, D. Schulte, and N. Tog, eds., *A Multi-TeV linear collider based on CLIC technology: CLIC Conceptual Design Report* (CERN, 2012).

[4] A. Anders, Plasma Sources Science and Technology **21**, 035014 (2012).

[5] A. Navitski, S. Lagotzky, D. Reschke, X. Singer, and G. Müller, Physical Review Special Topics-Accelerators and Beams **16**, 112001 (2013).

[6] T. Muranaka, K. Leifer, T. Blom, and V. Ziemann, *In-situ Experiments of Vacuum Discharge using Scanning Electron Microscopes*, Tech. Rep. (2011).

[7] K. Nagaoka, H. Fujii, K. Matsuda, M. Komaki, Y. Murata, C. Oshima, and T. Sakurai, Applied surface science **182**, 12 (2001).

[8] R. Little and W. Whitney, Journal of Applied Physics **34**, 2430 (1963).

[9] A. Descoeudres, T. Ramsvik, S. Calatroni, M. Taborelli, and W. Wuensch, Phys. Rev. ST-Accel. Beams **12**, 032001 (2009).

[10] H. Timko, M. Aicheler, P. Alknes, S. Calatroni, A. Oltedal, A. Toerklep, M. Taborelli, W. Wuensch, F. Djurabekova, and K. Nordlund, Physical Review Special Topics-Accelerators and Beams **14**, 101003 (2011).

[11] N. C. Shipman, *Experimental study of DC vacuum breakdown and application to high-gradient accelerating structures for CLIC*, Ph.D. thesis, The University of Manchester (2014).

[12] S. Lagotzky, G. Müller, P. Serbun, S. Calatroni, and T. Muranaka, in *WEPME005* (2014) p. 3.

[13] R. Latham, *High Voltage Vacuum Insulation: Basic Concepts and Technological Practice* (Elsevier Science, 1995).

[14] A. Degiovanni and W. Wuensch, "Comparison of the conditioning of high gradient accelerating structures," (2015), Submitted to PRST-AB.

[15] A. S. Pohjonen, S. Parviainen, T. Muranaka, and F. Djurabekova, Journal of Applied Physics **114**, 033519 (2013).

[16] H. Häkkinen, J. Merikoski, M. Manninen, J. Timonen, and K. Kaski, Physical review letters **70**, 2451 (1993).

[17] L. Wang and P. Clancy, Surface Science **473**, 25 (2001).

[18] C.-H. Lam, C.-K. Lee, and L. M. Sander, Physical review letters **89**, 216102 (2002).

[19] P. Zhang, X. Zheng, S. Wu, J. Liu, and D. He, Vacuum **72**, 405 (2004).

[20] A. Kara, O. Trushin, H. Yildirim, and T. S. Rahman, Journal of Physics: Condensed Matter **21**, 084213 (2009).

[21] G. Nandipati, A. Kara, S. I. Shah, and T. S. Rahman, Journal of Computational Physics **231**, 3548 (2012).

[22] J. B. Hannon, C. Klünker, M. Giesen, H. Ibach, N. C. Bartelt, and J. C. Hamilton, Physical review letters **79**, 2506 (1997).

[23] C. Mottet, R. Ferrando, F. Hontinfinde, and A. Levi, Surface science **417**, 220 (1998).

[24] M. I. Larsson, Physical Review B **64**, 115428 (2001).

[25] G. Henkelman and H. Jónsson, The Journal of Chemical Physics **115**, 9657 (2001).

[26] A. Karim, A. N. Al-Rawi, A. Kara, T. S. Rahman, O. Trushin, and T. Ala-Nissila, Physical Review B **73**, 165411 (2006).

[27] J. Frantz, M. Rusanen, K. Nordlund, and I. Koponen, Journal of Physics: Condensed Matter **16**, 2995 (2004).

[28] W. Liang, M. Zhou, and F. Ke, Nano Letters **5**, 2039 (2005).

[29] H. S. Park, K. Gall, and J. A. Zimmerman, Physical Review Letters **95**, 255504 (2005).

[30] M. Toimil Molares, A. Balogh, T. Cornelius, R. Neumann, and C. Trautmann, Applied physics letters **85**, 5337 (2004).

[31] L. Rayleigh, in *Proc. R. Soc. London*, Vol. 29 (1879) pp. 71–97.

[32] K. Zhao, R. Averback, and D. G. Cahill, Applied physics letters **89**, 053103 (2006).

[33] F. Atamny and A. Baiker, Surface science **323**, L314 (1995).

[34] K. A. Fichthorn and W. H. Weinberg, The Journal of Chemical Physics **95**, 1090 (1991).

[35] A. B. Bortz, M. H. Kalos, and J. L. Lebowitz, Journal of Computational Physics **17**, 10 (1975).

[36] W. M. Young and E. W. Elcock, Proceedings of the Physical Society **89**, 735 (1966).

[37] G. Mills and H. Jónsson, Physical review letters **72**, 1124 (1994).

[38] G. Mills, H. Jónsson, and G. K. Schenter, Surface Science **324**, 305 (1995).

[39] K. Nordlund, M. Ghaly, R. S. Averback, M. Caturla, T. D. de La Rubia, and J. Tarus, Physical Review B **57**, 7556 (1998).

[40] M. Ghaly, K. Nordlund, and R. S. Averback, Philosophical Magazine A **79**, 795 (1999).

[41] K. Nordlund, Computational materials science **3**, 448 (1995).

[42] M. S. Stave, D. E. Sanders, T. J. Raeker, and A. E. DePristo, The Journal of Chemical Physics **93**, 4413 (1990).

[43] S. B. Sinnott, M. S. Stave, T. J. Raeker, and A. E. DePristo, Physical Review B **44**, 8927 (1991).

[44] L. Vitos, A. Ruban, H. L. Skriver, and J. Kollar, Surface Science **411**, 186 (1998).

[45] W. Tyson and W. Miller, Surface Science **62**, 267 (1977).

[46] F. R. De Boer, W. Mattens, R. Boom, A. Miedema, and A. Niessen, (1988).

[47] F. Granberg, S. Parviainen, F. Djurabekova, and K. Nord-lund, Journal of Applied Physics **115**, 213518 (2014).

[48] J. Hook and H. Hall, *Solid State Physics*, Manchester Physics Series (Wiley, 2013).

[49] F. Soisson and C.-C. Fu, Physical Review B **76**, 214102 (2007).

[50] E. Vincent, C. Becquart, C. Pareige, P. Pareige, and C. Domain, Journal of Nuclear Materials **373**, 387 (2008).

[51] N. Castin, M. I. Pascuet, and L. Malerba, The Journal of chemical physics **135**, 064502 (2011).

[52] V. Jansson and L. Malerba, Journal of Nuclear Materials **443**, 274 (2013).

[53] See Supplemental Material at [URL will be inserted by publisher] for an animation of the flattening process in KMC and MD.

[54] W. Haynes, *CRC Handbook of Chemistry and Physics, 95th Edition* (CRC Press, 2014).

[55] T. Müller, K.-H. Heinig, and B. Schmidt, Materials Science and Engineering: C **19**, 209 (2002).

[56] H. Huang, G. H. Gilmer, and T. D. de la Rubia, Journal of Applied Physics **84**, 3636 (1998).